Unrevealed roles of extracellular enolase-1 (ENO1) in promoting glycolysis and pro-cancer activities in multiple myeloma via hypoxia-inducible factor 1α

I-CHE CHUNG[1], WEI-CHING HUANG[1], YUNG-TSANG HUANG[1],
MAO-LIN CHEN[1], AN-WEI TSAI[1], PEI-YU WU[2] and TA-TUNG YUAN[1]

[1]Department of Research and Development, HuniLife Biotechnology, Inc., Neihu, Taipei 114;
[2]Department of Manufacturing, TFBS Bioscience, Inc., Taipei 221, Taiwan, R.O.C.

Abstract. The involvement of enolase-1 (ENO1), intracellularly or extracellularly, has been implicated in cancer development. Moreover, anticancer activities of an ENO1-targeting antibody has demonstrated the pathological roles of extracellular ENO1 (surface or secreted forms). However, although ENO1 was first identified as a glycolytic enzyme in the cytosol, to the best of our knowledge, extracellular ENO1 has not been implicated in glycolysis thus far. In the present study, the effects of extracellular ENO1 on glycolysis and other related pro-cancer activities were investigated in multiple myeloma (MM) cells *in vitro* and *in vivo*. Knockdown of ENO1 expression reduced lactate production, cell viability, cell migration and surface ENO1 expression in MM cells. Notably, addition of extracellular ENO1 protein in cancer cell culture enhanced glycolytic activity, hypoxia-inducible factor 1-α (HIF-1α) expression, glycolysis-related gene (GRG) expression and pro-cancer activities, such as cell migration, cell viability and tumor-promoting cytokine secretion. Consistently, these extracellular ENO1-induced cellular effects were inhibited by an ENO1-specific monoclonal antibody (mAb). In addition, extracellular ENO1-mediated glycolysis, GRG expression and pro-cancer activities were also reduced by HIF-1α silencing. Lastly, administration of an ENO1 mAb reduced tumor growth and serum lactate levels in an MM xenograft model. These results suggested that extracellular ENO1 (surface or secreted forms) enhanced a HIF-1α-mediated glycolytic pathway, in addition to its already identified roles. Therefore, the results of the present study highlighted the therapeutic potential of ENO1-specific antibodies in treating MM, possibly via glycolysis inhibition, and warrant further studies in other types of cancer.

Introduction

Enolase-1 (ENO1) is a multifunctional protein (1), which mainly acts as a glycolytic enzyme in the cytosol to catalyze the conversion of 2-phospho-D-glycerate to phosphoenolpyruvate during aerobic glycolysis (2). Cancer cells undergo a metabolic shift to an aerobic glycolytic phenotype (termed the Warburg effect) during tumorigenesis, which provides cancer cells with survival advantages (3). This metabolic shift can be caused by an upregulation in ENO1 expression followed by enhanced conversion of pyruvate into lactate (4,5). ENO1 is also expressed on the cell surface where it acts as a plasminogen receptor under certain circumstances (6), which helps sequester circulating plasminogen to facilitate its activation. Resulting from proteolytic processing from plasminogen, plasmin acts as a potent extracellular serine protease specialized in the degradation of extracellular matrix. Owing to this ability, cells armed with plasminogen receptors would be able to harness the ability of plasmin for migration or invasion. Moreover, it has been reported that surface ENO1 promotes infiltration of immune cells (7) and metastasis of cancer cells (8) via its plasminogen-activating ability (9).

Upregulation of ENO1 has been observed in multiple cancer types, including multiple myeloma (MM) and prostate, lung and pancreatic neoplasms, and was often associated with poor prognosis (10-12). MM is a malignancy of plasma cells originating in the bone marrow, and is the second most common hematologic malignancy worldwide and in the United States after non-Hodgkin lymphoma (13). Despite the approval of novel therapeutics for MM, such as proteasome inhibitors (bortezomib) (14), immunomodulatory drugs (lenalidomide) (15) and monoclonal antibodies (daratumumab) (16), the treatment options remain limited for patients with relapsed refractory MM. Therefore, novel, safe and cost-effective treatments are still in urgent need. Ray *et al* (11) found a significantly higher *ENO1* gene expression level in patients with MM compared with the control subjects. Moreover, the level of *ENO1* gene expression was inversely correlated with the overall survival of patients with MM. ENO1 protein expression on the surface of MM cells was also confirmed (11). Since blocking surface ENO1 with antibodies has been demonstrated to be an effective anti-invasive/metastasis strategy for tumor progression in lung, pancreatic and cervical cancer (17-20), it was hypothesized that ENO1 could be a favorable therapeutic target for MM using our propriety ENO1-specific monoclonal antibody (mAb).

It was previously reported by the authors that an ENO1 mAb could attenuate tumor growth in prostate cancer (PCa) xenografts via disrupting the tumor microenvironment (TME) (12). Yu *et al* (21) also demonstrated that secreted ENO1 in the TME promoted PCa cell migration and metastasis. In addition, Ray *et al* (11) reported that co-culture of MM cells with plasmacytoid dendritic cells (pDCs) in the TME increased ENO1 expression on the MM cells. After treatment with an ENO1 inhibitor, pDCs acquired enhanced abilities of pDC-triggered T and NK cell-mediated anti-MM activity, which suggested a contribution of ENO1 to MM progression in the bone marrow TME. In addition, elevated lactate production in MM cells and the TME also contributes to the survival of MM cells (22). Evidence has also indicated that cell metabolic reprogramming necessitated cancer cells to upregulate the expression of key regulators of the glycolytic pathway, such as glucose transporter 1 (GLUT1), hexokinase 2 (HK2), phosphofructokinase (PFK) and ENO1 (23).

ENO1 was first recognized as one of the major regulators of glycolysis and its enzymology has been well studied. Subsequently, the 'moonlighting' functions of surface ENO1 have been gradually revealed in addition to the 'main' function (glycolysis) of intracellular ENO1, of which 'moonlighting' and 'main' are defined solely according to the time of discovery (10). Notably, the multiple functions of ENO1 have all been suggested to be involved in cancer development (24). However, to the best of our knowledge, it has not yet been addressed how ENO1 allocates the 'main' and 'moonlighting' duties to its intracellular and extracellular (surface or secreted) forms and how these duties are regulated. Therefore, in the present study, it was first determined whether extracellular ENO1 is involved in glycolysis regulation despite only cytosolic ENO1 being implicated in glycolysis thus far. Secondly, whether extracellular ENO1 could regulate glycolysis along with pro-cancer activities in MM cells was investigated. Lastly, a humanized ENO1-specific antibody was used to validate the role of extracellular ENO1 in glycolysis and tumor growth *in vivo*. To the best of our knowledge, this is the first study to explore the possibility that extracellular ENO1 (surface or secreted) could regulate glycolysis in cancer cells. The results of the present study may therefore shed light on the basic biology of ENO1 and the development of potential therapeutics for cancer.

Materials and methods

Human tissue array. An MM tissue array was obtained from TissueArray.com (formerly US Biomax, Inc.) (cat. no. BM483d), which contained 10 cases of plasma cell neoplasms and 11 bone marrow tissue (samples from the non-bone tumors in the chest surgery), with duplicate cores per case. Full ethical approval was granted for all aspects of the study and informed patient consent was obtained before tissue collection.

Animal studies. All animal studies were reviewed and approved by The Ethics Committee of TFBS Bioscience (Taipei, Taiwan). All animal procedures were performed according to approved protocols from the Institutional Animal Care and Use Committee (IACUC) of TFBS Bioscience (IACUC protocol no. TFBS2021-013). A total of 18 male 6-7-week-old BALB/c nude (nu/nu) mice (weighing 17-22 g) were purchased from BioLASCO Taiwan Co., Ltd. for the present study. The mice had free access to food and water and were kept on a 12/12-h light/dark cycle in the chambers under atmospheric conditions of 22°C and 30-60% humidity. Before inoculation, RPMI-8226 cells were washed with PBS and resuspended in serum-free RPMI-1640 medium and Matrigel (cat. no. 356231; Corning, Inc.) at a 1:1 ratio. The cells ($5x10^6/100$ μl) were subsequently implanted subcutaneously into the right flank of the mice. The subcutaneous tumor volume was determined according to the following formula: Tumor volume=(shorter diameter^2 x longer diameter)/2. After the tumor size reached >100 mm^3, the mice were randomized into three groups (n=6): Group 1 were administered PBS as a vehicle control; group 2 were administered a total of nine doses of ENO1 mAb; and group 3 were administered a total of five doses of ENO1 mAb. ENO1 mAb (30 mg/kg) was administered twice a week by intraperitoneal injection. Based on the tumorigenesis assessment, tumor weight >10% of the animal body weight was considered an indicator for animal sacrifice. To ameliorate the suffering of animals observed throughout the experimental studies, animals were euthanized by CO_2 inhalation (30-70% of the cage volume per min).

Cell culture. The RPMI-8226 [Bioresource Collection and Research Center (BCRC) no. 60384; RRID: CVCL_0014] and U266 (BCRC no. 60437; RRID: CVCL_0566) human MM cell lines and the PC-3 human PCa cell line (BCRC no. 60122, RRID: CVCL_0035) were obtained from the BCRC (Hsinchu, Taiwan). STR-PCR profiling was also conducted at the BCRC. The KMS-11 (cat. no. JCRB1179) cell line was obtained from the Japanese Collection of Research Bioresources Cell Bank (Osaka, Japan). The cells were cultured in RPMI-1640 (Gibco; Thermo Fisher Scientific, Inc.) supplemented with 10% fetal bovine serum (FBS; Gibco; Thermo Fisher Scientific, Inc.)

and 50 U/ml penicillin-streptomycin (Gibco; Thermo Fisher Scientific, Inc.) at 37˚C under 5% CO_2. For the evaluation of the effects of recombinant ENO1 on lactate production, lactate dehydrogenase (LDH) activity and the expression levels of candidate genes, RPMI-8226 cells were cultured in RPMI-1640 containing 2% FBS during treatment.

Reagents. Genes encoding human ENO1 proteins, including ENO1-wild-type (WT), ENO1-S40A and ENO1-D245R, were cloned into a pTrcHis vector, in which the expression of the transgene was isopropyl-β-D-thiogalactoside-inducible. The expression of recombinant ENO1 proteins in *Escherichia coli* and subsequent purification were performed by Leadgene Biomedical, Inc. (Tainan, Taiwan). The ENO1 proteins were suspended in 1X PBS containing 7 mM $MgSO_4$ and 2% trehalose, pH 7.2. Production of the proprietary ENO1 mAb by HuniLife was previously described (12). The ENO1 mAb was a humanized IgG1 antibody and cross reactive to both human and mouse ENO1, but was not reactive to ENO2 and ENO3. Human IgG1 (hIgG1; cat. no. HG1K; Sino Biological, Inc.) and anti-*Klebsiella pneumoniae* (hIgG1 backbone; provided by Dr Shih-Chong Tsai, Development Center for Biotechnology, Taipei, Taiwan) antibodies were used as isotype controls in the *in vitro* and *in vivo* studies, respectively. Recombinant human TNF-α protein (cat. no. 300-01A) was purchased from PeproTech, Inc. The nuclear factor-κB (NF-κB) inhibitor, BAY11-7085 (cat. no. sc-202490), was purchased from Santa Cruz Biotechnology, Inc.

Immunohistochemistry. All tissues were fixed in 10% neutral buffered formalin at room temperature for 24 h, dehydrated with gradient ethanol, cleared with xylene, and embedded in paraffin. MM tissue array sections (5-μm thick) were deparaffinized using two sequential 5 min washes in fresh xylene at room temperature, then gradually rehydrated in graded ethanol of 100, 95, 80, 70 and 50% and distilled water at room temperature for 3 min each. Heat-induced epitope retrieval was performed with 0.02 M Tris-EDTA (pH 9.0) using a microwave for 20 min. Endogenous peroxidase activity was quenched then tissues were stained with primary antibody against ENO1 (1:500; cat. no. ab227978; Abcam) or isotype control antibody (1:500; cat. no. ab172730; Abcam) at 4˚C overnight. The tissue slides were subsequently incubated with HRP-conjugated secondary antibody (1:1,000; cat. no. 7074; Cell Signaling Technology, Inc.) for 30 min at room temperature. Then, the DAB reaction was performed until the desired staining was achieved. The slides were then mounted after tissues were counterstained with hematoxylin. Whole images of each core were acquired using a Nikon microscope (Nikon Instruments) and the positively stained area (%) of each image was quantified using Nikon NIS-Elements (BR) software (Nikon Instruments Inc.).

RNA interference (RNAi). The ENO1 (Shanghai GenePharma Co., Ltd.) and HIF-1α (cat. no. AM51331; Invitrogen; Thermo Fisher Scientific, Inc.) siRNA sequences were as follows: si-ENO1 #1 sense, 5'-CGUACCGCUUCCUUAGAACUUTT-3' and antisense, 5'-AAGUUCUAAGGAAGCGGUACGTT-3'; si-ENO1 #2 sense 5'-GAAUGUCAUCAAGGAGAAAUATT-3' and antisense, 5'-UAUUUCUCCUUGAUGACA

UUCTT-3'; si-HIF1A sense, 5'-GGGUAAAGAACAAAACACA-3' and antisense, 5'-UGUGUUUUGUUCUUUACCC-3'; and scramble siRNA sense 5'-UUCUCCGAACGUGUCACGUTT-3' and antisense, 5'-ACGUGACACGUUCGGAGAATT-3'. Cells were transfected with 50 nM dsRNA duplexes using RNAiMAX (cat. no. 13778; Invitrogen; Thermo Fisher Scientific, Inc.) according to the manufacturer's instructions. Briefly, RPMI 8226 ($5x10^5$), U266 ($5x10^5$) and PC-3 ($2x10^5$) cells were plated in 2.5 ml of culture medium per well of six-well plates, and then were transfected with dsRNA duplexes (50 nM) using RNAiMAX for 72 h at 37˚C under 5% CO_2, and then the ENO1-knockdown cells were used for subsequent experiments. For knockdown of HIF-1α, RPMI 8226 cells were transfected again for another 24 h following the first transfection using the same protocol as aforementioned.

ENO1 stable overexpression. The *ENO1* gene was inserted into the expression vector, pLenti-C-Myc-DDK-P2A-Puro (cat. no. RC205494L3; OriGene Technologies, Inc.). KMS-11 cells were plated at $8x10^5$ cells in 2 ml of culture medium per well of six-well plates, and then were transfected with ENO1 expressing plasmid (4 μg) using Avalanche Transfection Reagent (cat. no. EZT-RPMI-1; EZ Biosystems™) for 5 h at 37˚C under 5% CO_2, followed by adding 0.5 ml of culture medium. Those cells stably overexpressing ENO1 (Myc/DDK-tagged) were selected with puromycin (2 μg/ml) for >2 weeks. Mock cells treated with transfection reagent alone were used as the control group. The efficacy of stable ENO1 overexpression was detected by immunoblotting analysis.

Flow cytometry detection of cell surface ENO1. ENO1-knockdown RPMI-8226 and U266 cells were stained for 30 min at room temperature with LIVE/DEAD Fixable Near-IR (775) (cat. no. L34975; Invitrogen; Thermo Fisher Scientific, Inc.), and then washed twice in PBS at 300 x g for 5 min. Cells were further incubated with Fc-block receptor (cat. no. 130-059901; Miltenyi Biotech, Inc.) for 10 min at 4˚C and then washed once in cold Stain Buffer (cat. no. 554656; BD Biosciences) at 300 x g for 5 min. Cells were stained with ENO1 (1:50; cat. no. H00002023-M01; Abnova) or isotype-matched mouse IgG1 (1:50; cat. no. 401402; Biolegend, Inc.) antibodies for 30 min at 4˚C, then washed twice in cold Stain Buffer at 300 x g for 5 min. Cells were then incubated with PE goat anti-mouse IgG (1:20; cat. no. 405307; Biolegend, Inc.) for 30 min at 4˚C, followed by washing twice in cold Stain Buffer at 300 x g for 5 min. After staining, the samples were resuspended in cold Stain Buffer and analyzed by a CytoFlex flow cytometer (Beckman Coulter, Inc.). Data were acquired using CytExpert 2.4 software and analyzed using Kaluza Analysis 2.1 Software (Beckman Coulter, Inc.). For each sample, $1x10^4$ cells were acquired. For analysis, the dead cells were first excluded with LIVE/DEAD Fixable Near-IR (775) Dead Cell Stain. Quantification of the surface ENO1 level [in mean fluorescence intensity (MFI)] was obtained by subtracting the MFI of the samples from the isotype control.

Antibody labelling assay for detection of cell surface ENO1. The method was as previously described (25), with modification. Briefly, ENO1-knockdown RPMI-8226 ($1x10^5$) and PC-3 ($0.5x10^5$) cells were harvested and washed twice with cold

PBS, fixed with 100 μl of 1% paraformaldehyde for 10 min on ice, and blocked with 200 μl of 1% BSA (cat. no. A9418; Sigma Aldrich; Merck KGaA) in PBS for 2 h at room temperature. After blocking, the cells were probed with ENO1 antibody (1:200; cat. no. H00002023-M01; Abnova) at 37°C for 1 h followed by HRP-conjugated anti-mouse secondary antibody (1:7,500; cat. no. 2076; Cell Signaling Technology, Inc.) at 37°C for 30 min. Final detection was performed using TMB substrate (cat. no. 5120; KPL; SeraCare; LGC Clinical Diagnostics), and the absorbance at 450 nm was determined using a microplate reader.

Immunoblotting analysis. RPMI-8226 or PC-3 lysates were prepared and subjected to immunoblotting analysis according to standard protocol. Briefly, cells were lysed in RIPA buffer (25 mM Tris-HCl, pH 7.6, 150 mM NaCl, 1% NP-40, 1% sodium deoxycholate, 0.1% SDS; cat. no. 89900; Thermo Fisher Scientific, Inc.) containing the 1X protease inhibitor cocktail (cat. no. 78340; Thermo Fisher Scientific, Inc.) on ice for 30 min, followed by centrifugation (13,500 x g for 10 min at 4°C). The protein concentrations were determined using a BCA protein assay kit (cat. no. 23225; Pierce; Thermo Fisher Scientific, Inc.). Proteins (30 μg) were resolved on a 10% SDS-PAGE gel, and then transferred to PVDF membranes (cat. no 10600023; Cytiva Life Sciences). The membranes were blocked in TBST (0.1% Tween-20 in TBS) with 5% non-fat dry milk for 1 h at room temperature, and then incubated overnight at 4°C with diluted primary antibodies in TBST with 5% non-fat dry milk. The membranes were then washed three times for 10 min each with TBST at room temperature on a gel rocker, and incubated with secondary antibodies coupled to HRP in TBST with 5% non-fat dry milk for 1 h at room temperature, followed by washing three times for 10 min each with TBST at room temperature on a gel rocker. The immunoreactive bands were detected with the ECL™ Select Western Blotting Detection Reagent (cat. no GERPN2235; Cytiva). The primary antibodies were as follows: ENO1 (1:2,000; cat. no. ab190365; Abcam), HIF-1α (1:1,000; cat. no. 610958; BD Biosciences), HK2 (1:2,000; cat. no. sc-130358; Santa Cruz Biotechnology, Inc.), 6-phosphofructo-2-kinase/fructose-2,6 biphosphatase 3 (PFKFB3; 1:2,000; cat. no. ab96699; Abcam), GLUT1 (1:5,000; cat. no. ab115730; Abcam), IκBα (1:2,000; cat. no. 9242; Cell Signaling Technology, Inc.), PHD2 (1:1,000; cat. no. sc-271835; Santa Cruz Biotechnology, Inc.) and GAPDH (1:5,000; cat. no. sc-32233; Santa Cruz Biotechnology, Inc.). The secondary antibodies were as follows: HRP-conjugated anti-mouse secondary antibody (1:5,000; cat. no. 2076; Cell Signaling Technology, Inc.) and HRP-conjugated anti-rabbit secondary antibody (1:5,000; cat. no. 7074; Cell Signaling Technology, Inc.).

Lactate and LDH assays. The levels of lactate in cell culture supernatant and intracellular LDH activity were measured using colorimetric lactate (cat. no. MET-5012; Cell Biolabs, Inc.) and LDH (cat. no. CK12-20; Dojindo Laboratories, Inc.) assay kits, respectively, according to the manufacturer's instructions. LDH activity results were normalized to the protein concentrations of the cell lysates, and the protein concentrations were determined using a BCA protein assay kit.

Cell viability and migration assays. Cell viability was measured using Cell Counting Kit-8 (cat. no. CK04-20; Dojindo Laboratories, Inc.) according to the manufacturer's instructions. Briefly, RPMI 8226 ($2x10^4$), U266 ($2x10^4$) and PC-3 ($1x10^4$) cells were plated in 100 μl of culture medium per well of 96-well plates. At 0, 24, 48 and 72 h, 10 μl of the Cell Counting Kit-8 solution was added to each well and incubated at 37°C for 2 h, and the absorbance at 450 nm was measured using a microplate reader. For the migration assay, cells were resuspended in medium supplemented with 2% FBS in the absence or presence of various concentrations of ENO1 mAb or control hIgG1. After adding 900 μl of medium containing 10% FBS to the bottom chamber of the migration plates, the coating-free insert (8-μm pores; cat. no. 3464; Corning, Inc.) was placed and the upper chamber was seeded with the treated cells. The cells were then allowed to migrate at 37°C for 18 h. The remaining cells in the upper chamber were removed and the cells in the bottom chamber were fixed with methanol for 10 min at room temperature, followed by staining with 1% crystal violet for an additional 2 h or overnight at room temperature. The insert was gently washed with PBS and dried. The bound crystal violet was eluted with 33% acetic acid and the absorbance at 590 nm was measured using a microplate reader.

Cytokine ELISA and measurement of enolase activity. Measurement of cytokine levels was performed using ELISA kits, including human vascular endothelial growth factor (VEGF; cat. no. DY293B-05; R&D Systems, Inc.), human interleukin 6 (IL-6; cat. no. DY206-05; R&D Systems, Inc.) and human transforming growth factor-β (TGF-β; cat. no. DY240-05; R&D Systems, Inc.), according to the manufacturer's instructions. The enolase activity of cell lysates or recombinant ENO1 (10 ng) were determined using an enolase activity colorimetric assay kit (cat. no. K691; BioVision, Inc.), according to the manufacturer's instructions.

Reverse transcription-quantitative PCR (RT-qPCR). Total RNA in the treated cells was extracted using an rSYNC RNA Isolation kit (cat. no. RS300; Geneaid Biotech Ltd.), and RT of the RNA was performed using an iScript™ cDNA Synthesis kit (cat. no. 1708891; Bio-Rad Laboratories, Inc.), according to the manufacturer's instructions. The primer sequences used to amplify the resulting cDNA were as follows: *HIF-1α* sense, 5'-AATTCTCAACCACAGTGCATTGTATGT-3' and antisense, 5'-CTTTGGTGAATAGCTGAGTCATTTTCA-3'; *HK2* sense, 5'-GAGTTTGACCTGGATGTGGTTGC-3' and antisense, 5'-CCTCCATGTAGCAGGCATTGCT-3'; *PFKFB3* sense, 5'-GGCAGGAGAATGTGCTGGTCAT-3' and antisense, 5'-CATAAGCGACAGGCGTCAGTTC-3'; *GLUT1* sense, 5'-TTGCAGGCTTCTCCAACTGGAC-3' and antisense, 5'-CAGAACCAGGAGCACAGTGAAG-3'; *ENO1* sense, 5'-AGTCAACCAGATTGGCTCCGTG-3' and antisense, 5'-CACAACCAGGTCAGCGATGAAG-3'; *c-Myc* sense, 5'-CCTGGTGCTCCATGAGGAGAC-3' and antisense, 5'-CAGACTCTGACCTTTTGCCAGG-3' and *ACTB* sense, 5'-CACCATTGGCAATGAGCGGTTC-3' and antisense, 5'-AGGTCTTTGCGGATGTCCACGT-3'. qPCR was performed on a BioRad CFX 384 using the PowerUp™ SYBR™ Green Master Mix (Applied Biosystems; Thermo Fisher Scientific, Inc.). The following thermal cycling

conditions were used: 50°C for 2 min; 95°C for 2 min; 95°C for 15 sec; and 60°C for 1 min for 40 cycles. The fold change in the expression of target genes were calculated by the relative quantification method (26). ΔCq values were obtained as follows: ΔCq=Cq of *ACTB*-Cq of the target gene. ΔΔCq values were then obtained as follows: ΔΔCq=ΔCq of the treated group-ΔCq of the control group. Fold change was calculated as $2^{-\Delta\Delta Cq}$, with control groups as 1-fold.

Measurement of glucose uptake. To evaluate glucose uptake, a colorimetric assay kit (cat. no. ab136955; Abcam) was used according to the manufacturer's instructions. Briefly, RPMI-8226 and U266 cells were treated with different concentrations of ENO1 mAb (1, 10 and 100 μg/ml) or hIgG1 (100 μg/ml) in RPMI-1640 media supplemented with 2% FBS for 48 h. Cells were then washed twice with PBS and cultured in glucose-free RPMI (Gibco; Thermo Fisher Scientific, Inc.) for 1 h. Subsequently, the cells were incubated in PBS for 40 min and then with 10 mM 2-deoxy-D-glucose (2-DG) for 20 min. Next, cells were washed three times with PBS to remove exogenous 2-DG, lysed with extraction buffer, freeze/thawed once and heated at 85°C for 40 min to degrade endogenous NAD(P), followed by centrifugation at 300 x g for 2 min at 4°C. The resulting supernatant was analyzed for 2-deoxy-D-glucose-6-phosphate content using a microplate reader at 412 nm. Cells treated with 100 μM phloretin were used as a positive control.

Measurement of plasminogen receptor activity of ENO1. RPMI-8226 and U266 cells were harvested and washed twice with PBS at 300 x g for 2 min, resuspended in PBS at 1×10^6 cells/ml and preincubated with various concentrations of ENO1 mAb (1, 10 and 100 μg/ml) or hIgG1 (100 μg/ml) at 37°C for 1 h, followed by treatment with 40 mM human Glu-plasminogen (cat. no. 528180; Sigma-Aldrich; Merck KGaA) for 1 h. After incubation, the cells were washed with PBS three times and resuspended in 100 μl PBS containing 1.5 μM tissue plasminogen activator (tPA) (cat. no. 612200; Sigma Aldrich; Merck KGaA) and 0.1 mM plasmin chromogenic substrate, Chromogenix S-2251 (cat. no. S820332; DiaPharma), at 37°C for 2.5 h. The plasminogen receptor activity (plasmin activation) was determined by measuring the absorbance at 405 nm.

Statistical analysis. All statistical analyses were performed using SPSS 18.0 (SPSS, Inc.). The data are presented as the mean ± SEM from at least three separate experiments. Differences between two individual experiments were compared using two-tailed unpaired Student's t-tests (Fig. 1B) or two-tailed paired Student's t-tests (Fig. S5B-F). Comparisons of multiple groups were performed by using one-way analysis of variance (ANOVA), and subsequent comparisons of individual groups were performed using Tukey's post hoc test. P<0.05 was considered to indicate a statistically significant difference.

Results

ENO1 is upregulated in the tumor tissues from patients with MM. A previous study demonstrated that *ENO1* gene expression was significantly higher in patients with MM
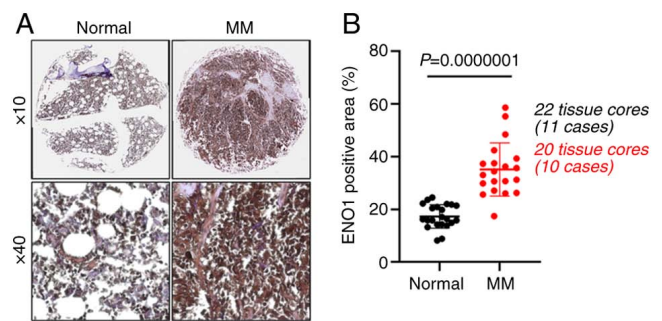

Figure 1. ENO1 expression in MM tumors is elevated compared with normal bone marrow tissues. A human MM tissue microarray (10 MM cases and 11 normal bone marrow cases, with duplicate cores per case) was used for immunohistochemical staining of ENO1. (A) Representative images were shown at x10 (upper panels) or x40 (lower panels) magnification. (B) Quantification of the ENO1-positively stained area. Each dot represents the result from one tissue core. The P-value was calculated with a two-tailed unpaired Student's t-test. ENO1, enolase-1; MM, multiple myeloma.

compared with control subjects (11). Therefore, in the present study, ENO1 protein expression was further examined using a human MM tissue array. The tissue samples included in tissue array (#BM483d) are summarized in Table SI. As revealed in Fig. 1, ENO1 protein expression was significantly higher in the bone marrow tissues from patients with MM compared with normal bone marrow tissues. These results were in agreement with the authors' previous study, in which upregulation of ENO1 in advanced grade human PCa tissues was also observed (12). These data led to a hypothesis that ENO1 may be involved in the pathogenesis of MM and PCa.

ENO1 knockdown attenuates lactate production, cell migration and cell viability. Upregulation of ENO1 has been found in various cancer types, where it enhances glycolysis and cell growth, migration and invasion (5,18,27,28), which are generally considered pro-cancer activities. However, the pathological roles of ENO1 in MM remain largely unknown. Therefore, in the present study, RNAi-mediated knockdown of ENO1 in human MM cells (RPMI-8226) was performed. This RNAi approach (by si-ENO1 #1 or #2) successfully reduced the expression of total cellular ENO1 protein in RPMI-8226 MM cells (Fig. 2A). In addition, a significant decrease in the levels of secreted lactate (the endpoint of glycolysis following the Warburg effect) from the ENO1-knockdown RPMI-8226 MM cells was observed (Fig. 2B). Moreover, knocking down ENO1 expression also inhibited cell migration (Fig. 2C) and cell viability (Fig. 2D). In another MM cell line (U266), cell viability was also reduced following knockdown of cellular ENO1 protein expression (Fig. 2G and H). In addition to MM, PCa cells have also been previously reported to exhibit the Warburg effect, where glycolysis was preferentially used for cell growth (29,30). Therefore, the same RNAi-mediated knockdown of ENO1 expression was applied to the PC-3 human PCa cells (Fig. S1A). Consistently, ENO1 knockdown also decreased lactate production (Fig. S1B), migration (Fig. S1C) and viability (Fig. S1D) of PC-3 cells. Taken together, these results suggested that ENO1 was required for glycolysis, motility and viability of MM and PCa cells.
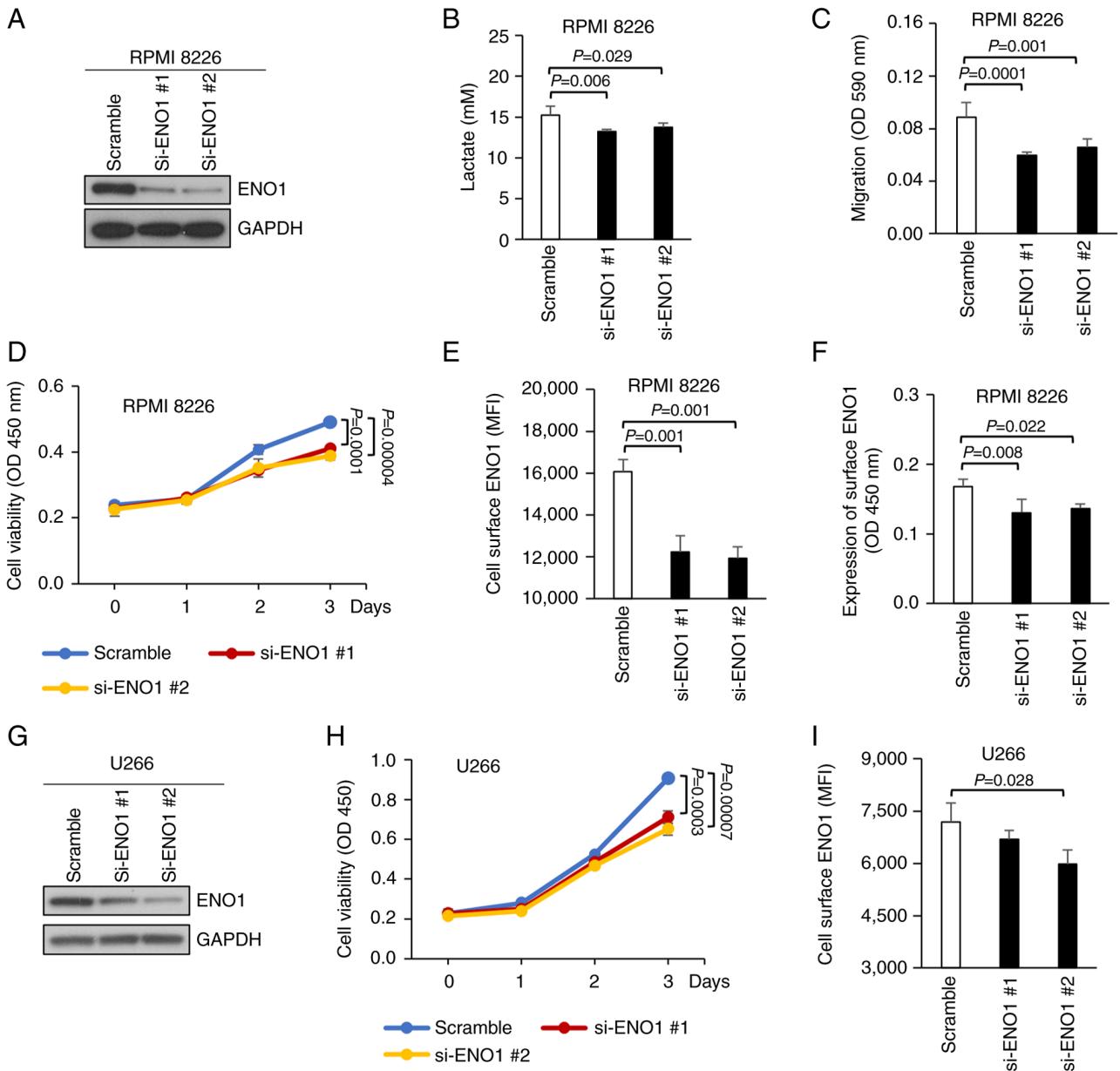
Figure 2. ENO1 knockdown attenuates lactate production, cell migration, cell viability and surface ENO1 expression. RPMI-8226 and U266 cells were transfected with ENO1-targeting siRNA (si-ENO1 #1 or #2) or control siRNA (scramble sequence) for 72 h, and ENO1 depletion efficiency was confirmed by (A and G) western blotting. GAPDH served as the loading control. (B) ENO1-knockdown RPMI 8226 cells were cultured for an additional 48 h, and then the supernatant was collected for determination of lactate levels. (C) Transwell migration assay, (D and H) cell viability assays, and measurement of cell surface ENO1 by (E and I) flow cytometry and (F) an antibody labeling assay were performed. All results are presented as the mean ± SD of three independent experiments. P-values were calculated with one-way ANOVA (with Tukey's post hoc test). ENO1, enolase-1; siRNA, small interfering RNA.

Extracellular ENO1 enhances glycolysis and pro-cancer activities. The enzymatic role of cytosolic ENO1 in glycolysis is well-known. Therefore, the aforementioned reduced lactate levels and biological effects of ENO1 knockdown, which reduced the total cellular expression of ENO1, were not surprising (Figs. 2A, G and S1A). However, knockdown of ENO1 also simultaneously reduced the levels of surface (or membrane bound) ENO1 in MM and PCa cells, as detected by flow cytometry (Fig. 2E and I) and antibody labelling assays (Figs. 2F and S1E). Therefore, it was of interest to determine whether extracellular ENO1 (surface or secreted) was involved in the reduced glycolysis and related biological activities observed in the knockdown studies,

since ENO1 enzymatic activity had been considered to be exclusive to the cytosolic form thus far. To determine this, cells were treated with recombinant ENO1-WT. Notably, extracellular ENO1 dose-dependently increased the level of lactate secreted from RPMI-8226 cells, and this increase was ENO1-specific since it was attenuated by co-treatment with an ENO1-specific mAb (Fig. 3A). Consistently, recombinant ENO1 also significantly promoted intracellular LDH activity (P=0.028; Fig. 3A), which catalyzed the conversion of pyruvate to lactate in glycolysis. This enhanced LDH activity was reduced upon ENO1 mAb co-treatment, although this reduction was not statistically significant (Fig. 3A).
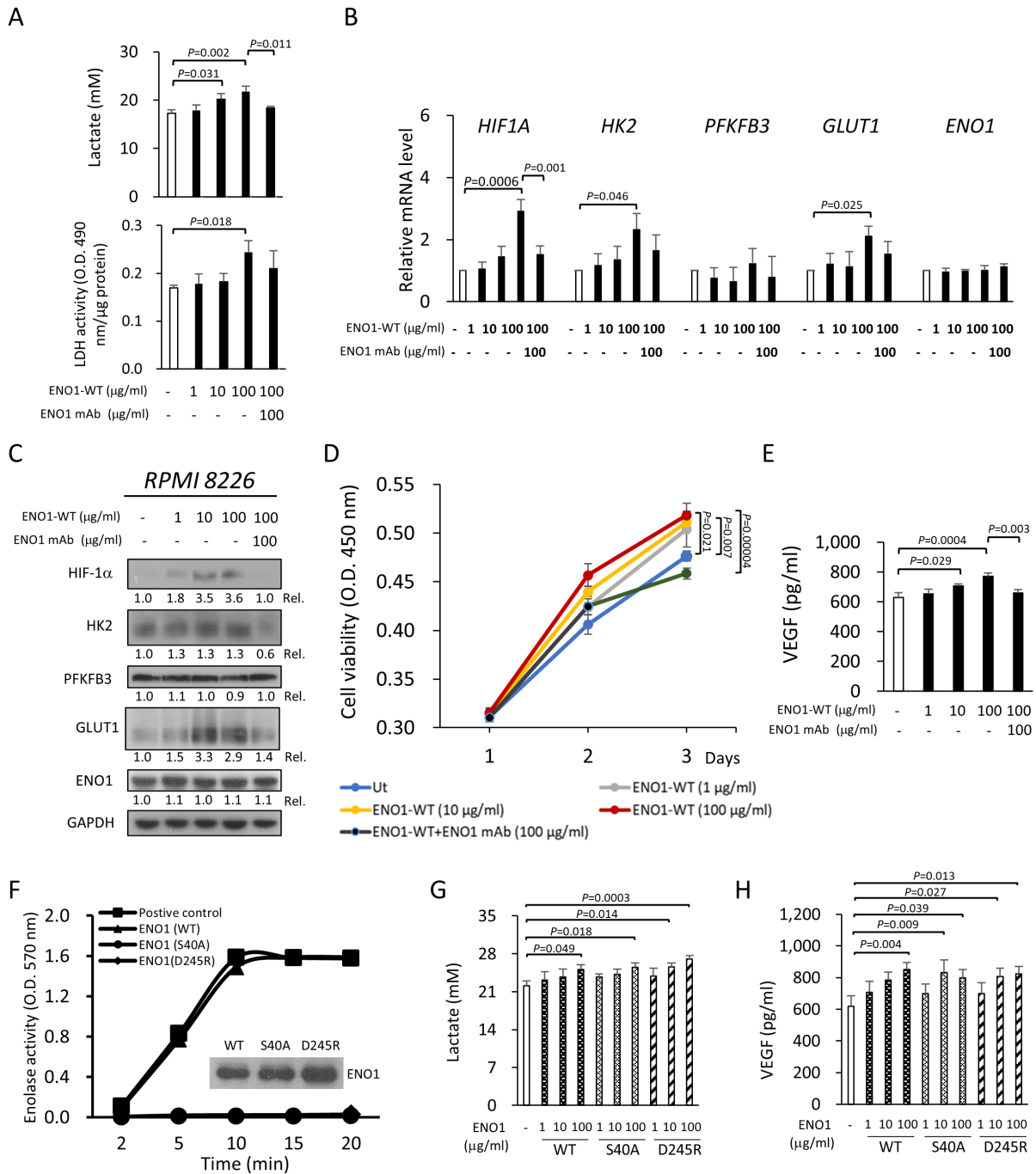
Figure 3. Extracellular ENO1 enhances glycolysis and pro-cancer activities. RPMI-8226 cells were treated with the indicated concentrations of recombinant ENO1-WT. The studies were conducted in the presence or absence of 100 μg/ml ENO1 mAb (also termed HuL001). (A) The lactate concentration in the culture medium (upper panel) and intracellular LDH activity (lower panel) were measured 48 h after ENO1-WT treatment. (B) The *HIF1A*, *HK2*, *PFKFB3*, *GLUT1* and *ENO1* mRNA levels were quantified by reverse transcription-quantitative PCR after 6 h of ENO1-WT treatment. (C) The HIF-1α, HK2, PFKFB3, GLUT1 and ENO1 protein levels were analyzed by immunoblotting after 24 h of ENO1-WT treatment. The amounts of studied proteins were first normalized with GAPDH, and the Rel was then calculated by comparing with the levels in the untreated cells, of which the value is set to 1.0. (D) Cell viability was measured using Cell Counting Kit-8. (E) Secretion of VEGF was measured by ELISA after 48 h of ENO1-WT treatment. (F) The enolase activity of ENO1-WT and two catalytically dead mutants, ENO1-S40A and ENO1-D245R, was measured. RPMI-8226 cells were treated with the indicated concentrations of ENO1-WT, ENO1-S40A and ENO1-D245R for 48 h. The (G) lactate and (H) VEGF concentrations in the culture medium were measured. All results are presented as the mean ± SD of three independent experiments. P-values were calculated with one-way ANOVA (with Tukey's post hoc test). ENO1, enolase-1; ENO1-WT, wild-type ENO1; GLUT1, glucose transporter 1; HIF1A or HIF-1α, hypoxia-inducible factor 1-α; HK2, hexokinase 2; LDH, lactate dehydrogenase; PFKFB3, 6-phosphofructo-2-kinase/fructose-2,6 biphosphatase 3; Rel., relative ratio; Ut, untreated; VEGF, vascular endothelial growth factor.

Next, the possible mechanism of this enhanced aerobic glycolysis by extracellular ENO1 was investigated. Gene expression levels of HIF-1α and glycolysis-related genes (GRGs) after treatment of cells with ENO1 protein were analyzed using RT-qPCR. Compared with the control,

ENO1-treated RPMI-8226 cells had higher *HIF1A*, *HK2* and *GLUT1* mRNA levels, which was not observed for *PFKFB3* and *ENO1* (Fig. 3B). Furthermore, the effects of extracellular ENO1 on the transcription of glycolysis-related genes were attenuated by ENO1 mAb (Fig. 3B). Consistently,

extracellular ENO1 also enhanced HIF-1α, HK2 and GLUT1 protein expression in RPMI-8226 cells, but not the protein expression of PFKFB3 and ENO1 (Fig. 3C). This increase in ENO1-induced protein expression was reduced by ENO1 mAb co-treatment. Since aerobic glycolysis is a hallmark of cancer, cell viability and the production of VEGF (a key mediator of angiogenesis) were also measured in MM cells following treatment with extracellular ENO1. Cell viability and VEGF production in RPMI-8226 cells were increased following ENO1 treatment, and were abrogated by ENO1 mAb co-treatment (Fig. 3D and E). Similar results were also obtained following treatment of PC-3 cells. ENO1 also increased the lactate production (Fig. S2A), intracellular LDH activity (Fig. S2B) and cell migration (Fig. S2C) of PC-3 cells, and these effects were attenuated by ENO1 mAb treatment. These data, for the first time (to the best of our knowledge), demonstrated that extracellular ENO1 enhanced glycolysis, possibly through a mechanism controlling the expression of HIF-1α and glycolysis-related proteins. The increase of glycolysis by extracellular ENO1 simultaneously enhanced cell viability, migration and VEGF production.

Although it was demonstrated that extracellular ENO1 enhanced glycolysis, it was of interest to determine whether its enzymatic activity was essential for extracellular ENO1-mediated glycolysis in the cytoplasm. For this purpose, two catalytically inactive ENO1 mutants (ENO1-S40A and ENO1-D245R) without enolase activity were generated (Fig. 3F). Subsequently, it was observed that mutant ENO1 proteins induced production of lactate (both ENO1-S40A and ENO1-D245R; Fig. 3G) and VEGF (both ENO1-S40A and ENO1-D245R; Fig. 3H) in RPMI-8226 cells, similar to ENO1-WT. In parallel, increased cell migration was also observed in PC-3 cells treated with ENO1-S40A and ENO1-D245R (Fig. S2D). Thus, the catalytic activity of extracellular ENO1 was not required for the enhancement of glycolysis and pro-cancer activities.

Extracellular ENO1 enhances glycolysis and pro-cancer activities via HIF-1α. It has been reported that HIF-1α regulates the expression of glycolysis-related genes, leading to lactate production and tumor progression (31). Therefore, whether extracellular ENO1 regulates glycolysis and pro-cancer activities through HIF-1α was further investigated. It was demonstrated that extracellular ENO1 upregulated the mRNA (Fig. 4A) and protein (Fig. 4B) levels of HIF-1α, HK2 and GLUT1 in RPMI-8226 cells, which was abrogated by knockdown of HIF-1α expression (with si-HIF1A) but not by control siRNA. Notably, knockdown of HIF-1α expression also inhibited extracellular ENO1-induced lactate secretion (Fig. 4C) and pro-cancer activities, such as increased IL-6 (a growth factor for MM; Fig. 4D), VEGF (Fig. 4E), cell viability (Fig. 4F) and cell migration (Fig. 4G). Although the reductions in ENO1-induced lactate secretion (P=0.067) and cell viability (P=0.425) were not statistically significant, a trend of reduction was observed. Taken together, these results suggested that the extracellular ENO1/HIF-1α axis enhanced glycolysis and pro-cancer activities in MM cells.

Since NF-κB and HIF-1α have been reported to play key roles in the pathogenesis of MM (32), the involvement of NF-κB activation in the extracellular ENO1/HIF-1α axis in

MM was next explored. As shown in Fig. 4B, degradation of IκBα (an obligatory step in NF-κB activation) following extracellular ENO1 administration was observed, which was reversed in the HIF-1α-knockdown cells. This suggested that HIF-1α may be involved in the extracellular ENO1-induced NF-κB activation. However, it was demonstrated that extracellular ENO1 upregulated HIF-1α protein levels, and this increase was not altered in the presence of an NF-κB inhibitor (BAY 11-7085), indicating that extracellular ENO1-induced HIF-1α upregulation was not regulated in a NF-κB-dependent manner (Fig. S3). Additionally, extracellular ENO1 enhanced the protein expression of HIF-1α. Furthermore, HIF-prolyl hydroxylase (PHD) is responsible for the degradation of HIF-1α under normal condition (23), thus it was investigated if PHD expression is regulated by extracellular ENO1. RPMI 8226 cells were treated with extracellular ENO1 followed by measurement of PHD2 protein (a main regulator of HIF-1). As demonstrated in Fig. S4, the levels of PHD2 protein were not altered in the presence of ENO1.

The aforementioned results demonstrated that glycolysis and pro-cancer activities were suppressed by ENO1 knockdown and promoted by extracellular ENO1 treatment. Thus, these observations were further investigated by increasing the overall expression of ENO1 in MM cells. The overexpressed ENO1 (Myc/DDK-tagged) protein level was observed in the KMS-11 MM cell line (oeENO1) compared with that of mock cells (Fig. S5A). Overexpression of ENO1 in the KMS-11 cells slightly increased the HIF-1α protein expression level compared with the mock cells, but an increase in GLUT1 and HK2 protein levels was not observed (Fig. S5A). However, a slight increase in lactate production (P=0.080) following ENO1 overexpression was observed (Fig. S5B). Interestingly, overexpression of ENO1 promoted certain pro-cancer activities, including cell viability (Fig. S5C) and migration (Fig. S5F), but had no impact on IL-6 (Fig. S5D) and VEGF (Fig. S5E) secretion levels.

ENO1 mAb reduces glycolytic activities. Following the results of the extracellular ENO1 studies (Figs. 3 and 4), it was of further interest to determine whether surface (or membrane bound) ENO1 could mediate glycolysis, using the proprietary HuniLife ENO1 mAb as an investigatory tool. Without the addition of ENO1 protein, it was demonstrated that ENO1 mAb treatment reduced the levels of secreted lactate in two MM cell lines (RPMI-8226 and U266) in a dose-dependent manner (Fig. 5A). To delineate the underlying mechanism, it was first revealed that ENO1 mAb did not directly affect total cellular enolase activity (Fig. 5B). However, it was demonstrated that ENO1 mAb decreased glucose uptake in RPMI-8226 and U266 cells in a dose-dependent manner, compared with the hIgG1 control (Fig. 5C). Moreover, the ENO1 mAb reduced the protein expression levels of HIF-1α, HK2 and PFKFB3 in RPMI-8226 cells, but did not affect the expression levels of GLUT1 and ENO1 (Fig. 5D). Similarly, ENO1 mAb significantly reduced lactate production in PC-3 cells following stimulation with TNF-α, which mimicked the inflammatory environment of advanced PCa tumors (Fig. S2F). Collectively, these results led to the hypothesis that cell surface ENO1 may be involved in controlling glycolytic flux in cancer cells.
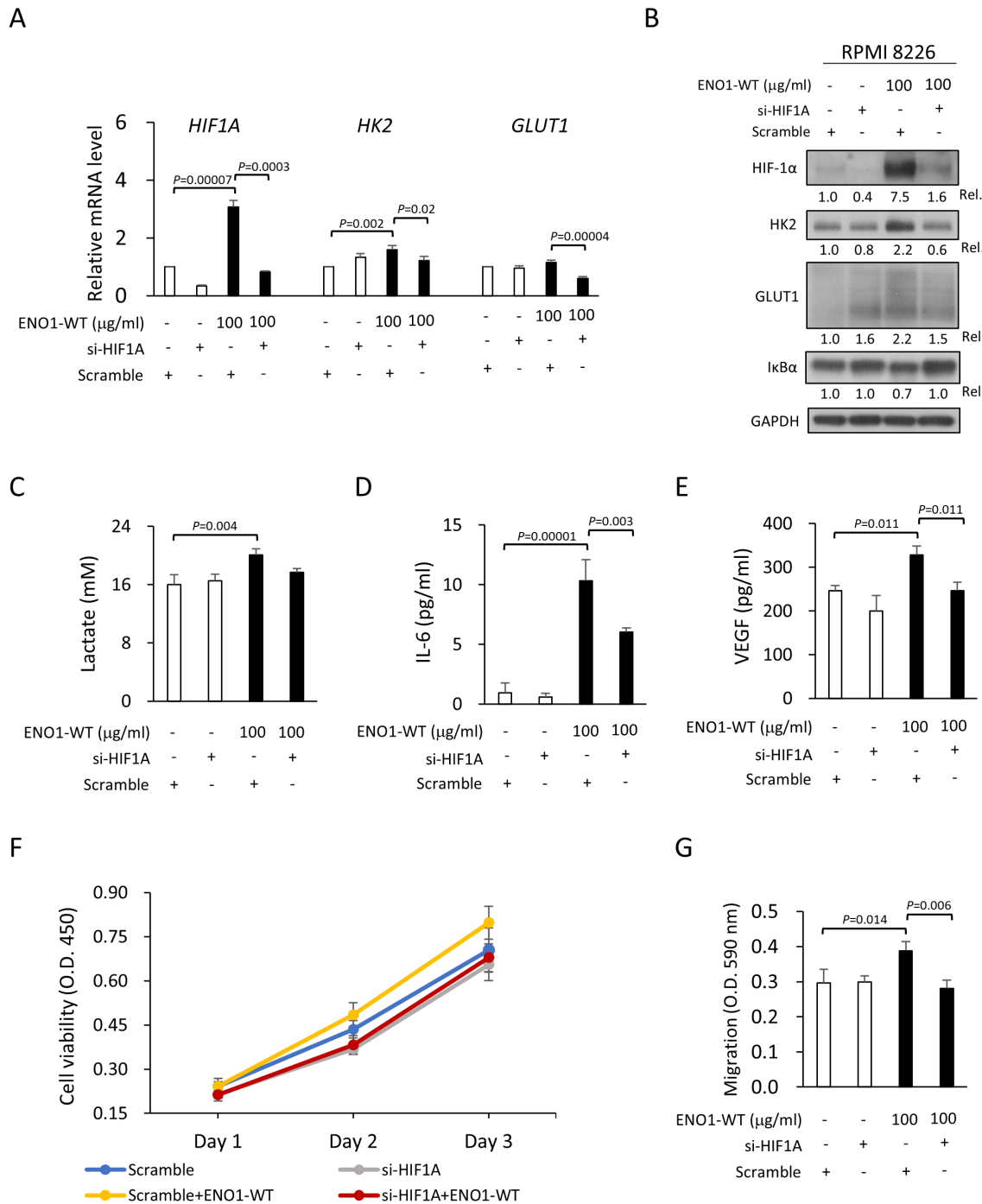
Figure 4. Extracellular ENO1 enhances glycolysis and pro-cancer activities through HIF-1α. RPMI-8226 cells were transfected with HIF-1α-targeting siRNA (si-HIF1A) or control siRNA (scramble sequence) for 96 h. (A) The *HIF1A*, *HK2* and *GLUT1* mRNA levels were quantified by reverse transcription-quantitative PCR after 6 h of treatment with or without 100 μg/ml ENO1-WT. (B) The HIF-1α, HK2, GLUT1 and IκBα protein levels and the (C) lactate, (D) IL-6 and (E) VEGF concentrations in the culture medium were measured 24 h after treatment with ENO1-WT. The amounts of studied proteins were first normalized with GAPDH, and then the Rel. was calculated by comparing with the scramble siRNA-treated cells, of which the value is set to 1.0. (F) Cell viability and (G) Transwell migration assays of RPMI-8226 cells with or without ENO1-WT treatment were performed following transfection with si-HIF1A or control siRNA. All results are presented as the mean ± SD of three independent experiments. P-values were calculated with one-way ANOVA (with Tukey's post hoc test). ENO1, enolase-1; ENO1-WT, wild-type ENO1; GLUT1, glucose transporter 1; HIF1A or HIF-1α, hypoxia-inducible factor 1-α; HK2, hexokinase 2; IL-6, interleukin 6; LDH, lactate dehydrogenase; Rel., relative ratio; siRNA, small interfering RNA; VEGF, vascular endothelial growth factor.

ENO1 mAb reduces cell viability, migration and cytokine production. In addition to the inhibition of glycolysis, the anti-cancer effects of the proprietary HuniLife ENO1 mAb on cell viability, cell migration and the production of tumor-secreted factors were further explored *in vitro*. It was demonstrated that the ENO1 mAb inhibited the viability of RPMI-8226 and

U266 cells by 18 and 25%, respectively (Figs. 5E and S6). The ENO1 mAb also inhibited the migration of RPMI-8226 cells in a dose-dependent manner (Fig. 5F). A similar inhibition of TNF-α-stimulated migration of PC-3 cells by ENO1 mAb was also observed (Fig. S2E). Cell surface ENO1 has been reported to be a receptor for activating plasminogen to stimulate
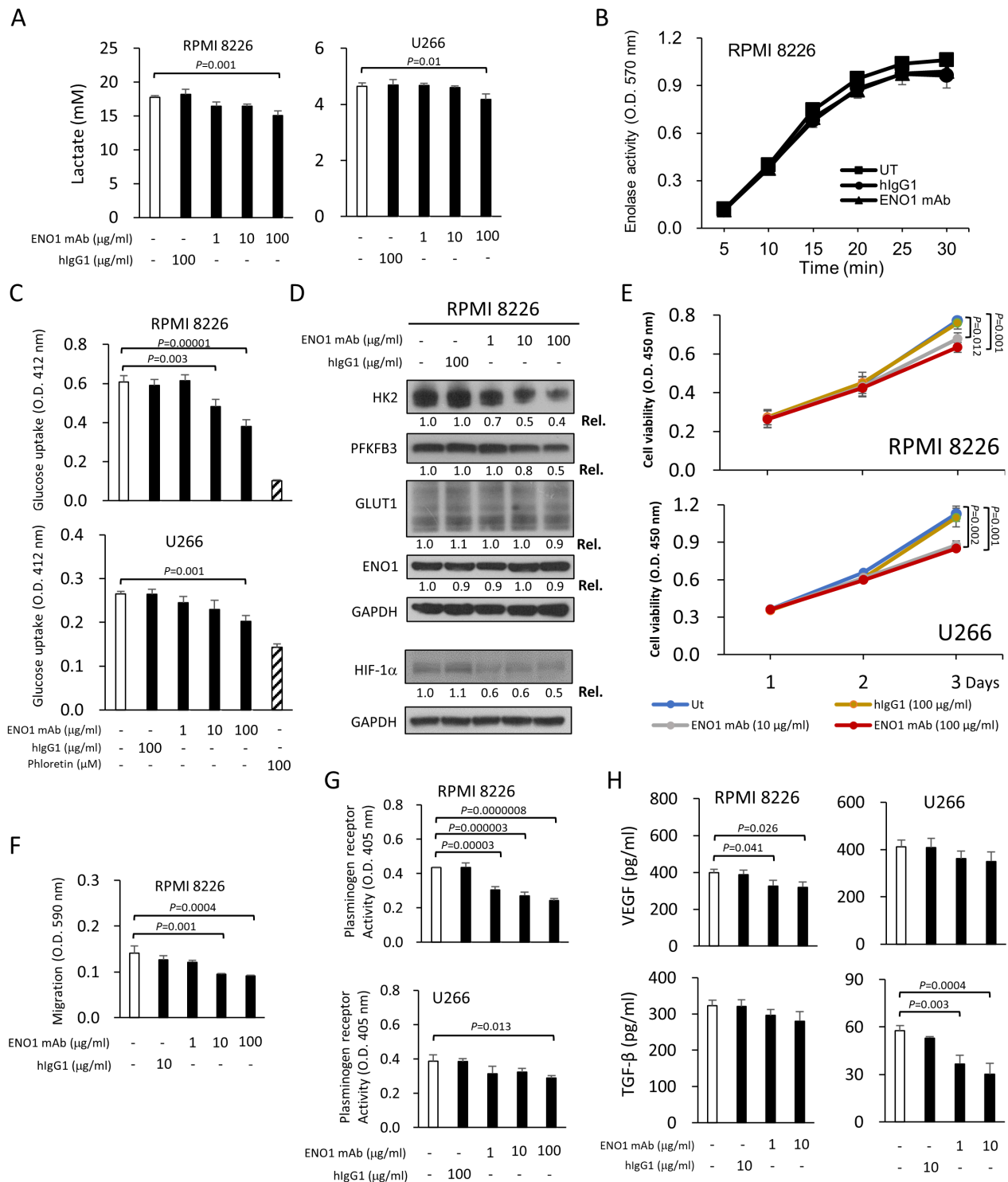
Figure 5. ENO1 mAb reduces glycolytic and pro-cancer activities. (A) The lactate concentrations in the culture medium, collected from ENO1 mAb-treated RPMI-8226 (left panel) and U266 (right panel) cells, were measured after 48 h of ENO1 mAb treatment. In all studies, hIgG1 at the indicated concentrations was included as a specificity control for ENO1 mAb. RPMI-8226 and U266 cells were treated with 100 μg/ml ENO1 mAb or 100 μg/ml hIgG1 for 48 h. (B) Enolase activity and (C) glucose uptake in lysates were further analyzed. Phloretin (a GLUT1 inhibitor) was added at 100 μM as a positive control to inhibit glucose uptake. (D) RPMI-8226 cells were treated with the indicated concentrations of ENO1 mAb or hIgG1 for 24 h. The HIF-1α, HK2, PFKFB3, GLUT1 and ENO1 protein levels were analyzed by immunoblotting. The amounts of studied proteins were first normalized with GAPDH, and then the Rel. was calculated by comparing with the untreated cells, of which the value was set to 1.0. (E) RPMI-8226 (upper panel) or U266 (lower panel) cells were treated with the indicated concentrations of ENO1 mAb or hIgG1. Cell viability was assessed 1, 2 or 3 days after treatment using the Cell Counting Kit-8. The OD 450 nm value was positively associated with the number of viable cells. (F) RPMI-8226 cells were treated with the indicated concentrations of ENO1 mAb or hIgG1. Cell migration was measured by Transwell assay after 18 h of treatment. (G) RPMI-8226 (upper panel) and U266 (lower panel) cells were treated with the indicated concentrations of ENO1 mAb or hIgG1 followed by measurement of the plasminogen receptor activity. (H) RPMI-8226 (left panels) or U266 (right panels) cells were treated with the indicated concentrations of ENO1 mAb or hIgG1 for 48 h. Supernatant was collected for determination of human VEGF (upper panel) and TGF-β (lower panel) levels by ELISA. All results are presented as the mean ± SD of three independent experiments. P-values were calculated with one-way ANOVA (with Tukey's post hoc test). ENO1, enolase-1; GLUT1, glucose transporter 1; HIF-1α, hypoxia-inducible factor 1-α; hIgG1, human IgG1; HK2, hexokinase 2; mAb, monoclonal antibody; PFKFB3, 6-phosphofructo-2-kinase/fructose-2,6 biphosphatase 3; Rel., relative ratio; TGF, transforming growth factor; Ut, untreated; VEGF, vascular endothelial growth factor.
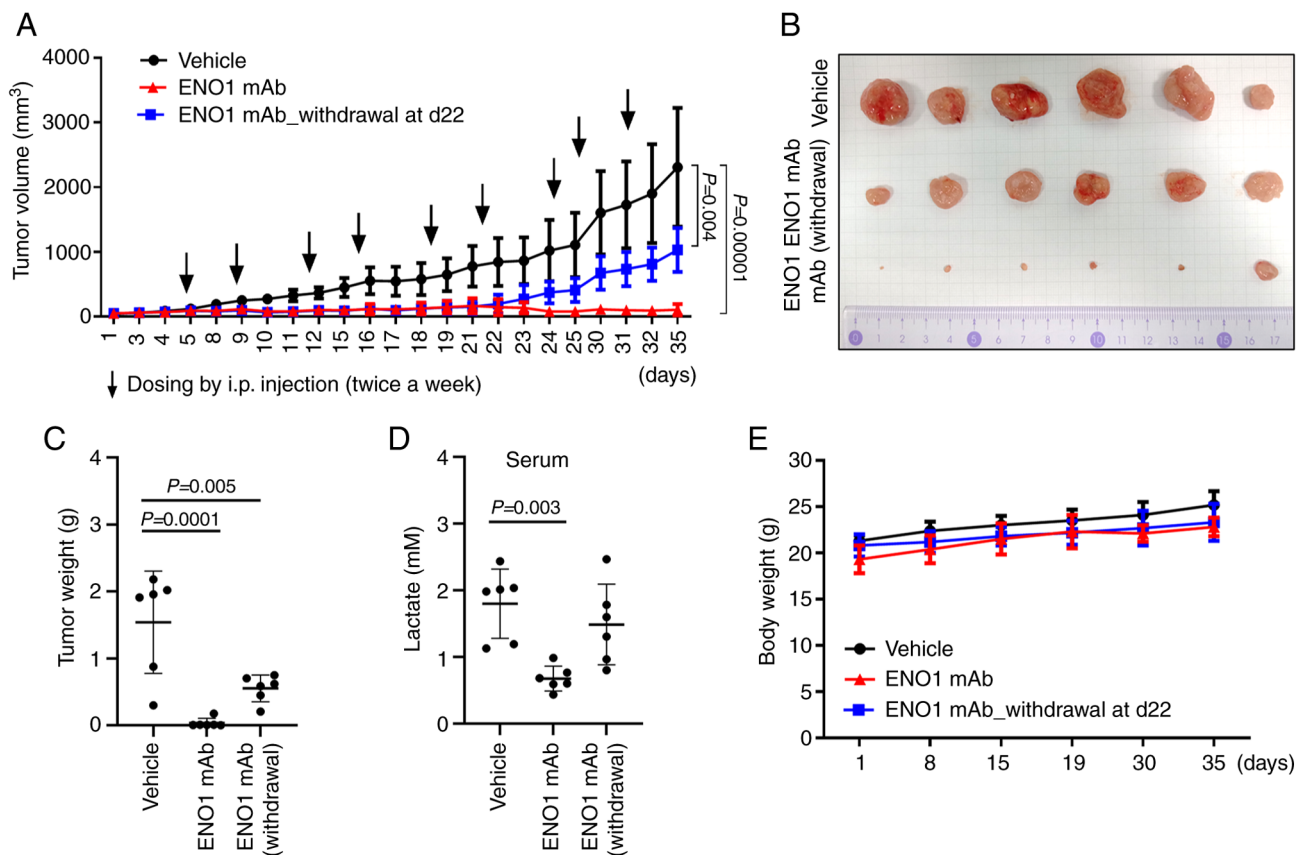
Figure 6. ENO1 mAb reduces tumor growth and glycolysis *in vivo* in a RPMI-8226 subcutaneous xenograft model. Male nude mice were subcutaneously implanted with RPMI-8226 cells and randomized when the tumor size reached >100 mm³ (n=6). ENO1 mAb (30 mg/kg) was intraperitoneally injected twice a week at the indicated time points. (A) Each data point represents the mean volume ± SD from the ENO1 mAb-treated, the withdrawing ENO1 mAb treated or vehicle control groups. Mice were sacrificed on day 35 and (B) representative images of excised tumors and the (C) tumor weight are shown. (D) Sera were collected for measurement of lactate concentration. (E) Mice body measurements were collected at the indicated time points. P-values were calculated with one-way ANOVA (with Tukey's post hoc test). ENO1, enolase-1; mAb, monoclonal antibody.

migration of cells (6). Consistently, a reduction in plasminogen receptor activity was observed in RPMI-8226 and U266 cells following treatment with ENO1 mAb (Fig. 5G). The secretion levels of VEGF and TGF-β (a key modulator of the TME) in these two MM cell lines were also reduced by administration of the ENO1 mAb (Fig. 5H). Although several ENO1-specific antibodies have also been reported to inhibit cancer invasiveness, metastasis and stemness (8,12,17-20), to the best of our knowledge, none have been investigated for their effects on glycolysis (the Warburg effect). In summary, the proprietary HuniLife ENO1 mAb demonstrated both an antiglycolytic and antitumor potential in MM and PCa cells (Figs. 5 and S2).

In addition, the alternative spliced nuclear isoform of ENO1, named c-myc promoter binding protein 1 (MBP-1), acts as a tumor suppressor (1). It was further determined whether ENO1 mAb is involved in the regulation of MBP-1 expression. RPMI-8226 cells were treated with ENO1 mAb followed by measuring MBP-1 protein levels. As revealed in Fig. S7A, the MBP-1 protein levels were not significantly altered in the presence of ENO1 mAb. Moreover, it has been reported MBP1 bound to the c-Myc promoter acts as a transcriptional suppressor (1). The *c-MYC* mRNA levels in RPMI-8226 cells upon the treatment of ENO1 mAb were therefore analyzed. The results indicated that ENO1 mAb had no significant impact on regulation of *c-Myc* transcription (Fig. S7B).

ENO1 mAb reduces tumor growth and glycolysis in a RPMI-8226 subcutaneous xenograft mouse model. It has previously been reported that the ENO1 mAb reduced tumor growth in PC-3 subcutaneous xenograft and intra-tibial implantation mouse models (12). Therefore, it was further investigated whether the ENO1 mAb could exert anticancer effects on MM cells *in vivo*. Nude mice were injected with RPMI-8226 cells, and the subcutaneous tumors were treated with 30 mg/kg ENO1 mAb twice a week. After nine doses in 35 days, both the tumor volume (Fig. 6A and B) and tumor weight (Fig. 6C) were reduced by ENO1 mAb treatment, compared with the vehicle control group. This reduction in tumor growth was attenuated when ENO1 mAb treatment was withdrawn from day 22. High serum lactate levels have been reported to be associated with poor prognosis and a reduced overall survival in patients with various types of cancer (33,34). Elevated lactate levels in mice were also associated with tumor growth in the present xenograft study (Fig. 6D). Notably, ENO1 mAb treatment reduced serum lactate levels in the tumor-bearing mice, and this reduction was abrogated upon withdrawing ENO1 mAb treatment. In addition, ENO1 mAb administration did not result in an apparent difference in body weight gain (Fig. 6E), which indicated minimal toxicity of ENO1 mAb treatment in animals. Moreover, hIgG1 isotype was included as a control in the present study, which did not have significant
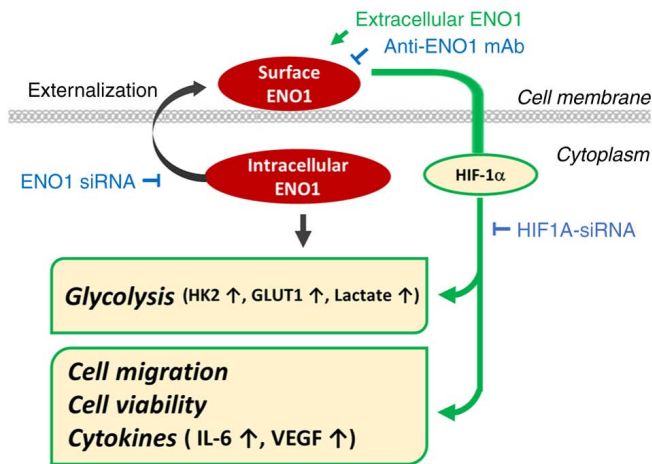
Figure 7. Schematic diagram summarizing the effects and possible mechanisms of extracellular ENO1 in regulating glycolysis and pro-cancer activities. Extracellular ENO1 may enhance glycolytic activity and glycolysis-related genes, including HK2 and GLUT1, through HIF-1α. Moreover, extracellular ENO1 also promoted HIF-1α-mediated pro-cancer activities, such as cell migration, cell viability and production of tumor-promoting cytokines. Consistently, these effects on cancer progression could be attenuated by the ENO1 antibody or ENO1 siRNA. ENO1, enolase-1; GLUT1, glucose transporter 1; HIF-1α, hypoxia-inducible factor 1-α; HK2, hexokinase 2; siRNA, small interfering RNA.

effects on the tumor volume (Fig. S8A and B), tumor weight (Fig. S8C), serum lactate levels (Fig. S8D) and body weight gain (Fig. S8E) in animals. A previous study indicated that drugs need to achieve systemic concentrations in the blood that permit adequate penetration and target binding into the tumor tissue (35). Based on the ENO1 concentration (1-100 μg/ml) studied *in vitro*, higher dose (30 mg/kg=625 μg/ml serum drug concentration) of ENO1 mAb than theoretically required was used to ensure sufficient drug distribution into tumor site *in vivo*. Moreover, it was determined that the half-life of proprietary ENO1 mAb was ~10 days in mice. In the MM subcutaneous xenograft studies, the frequency of ENO1 mAb administration was twice a week, to ensure there was a stable level of ENO1 mAb for the treatment duration in animals. Taken together, these results suggested that the ENO1 mAb could serve as a novel therapeutic by targeting glycolysis and associated pro-cancer activities in MM.

Discussion

ENO1 is a multifunctional protein with a 'main' function as a glycolytic enzyme in the cytosol and a 'moonlighting' function as a plasminogen receptor on the cell surface (10). Both the main and moonlighting roles of ENO1 have been implicated in cancer progression (24), but, to the best of our knowledge, there has not yet been a study to address the role of extracellular ENO1 in the context of glycolysis. Therefore, the present study was the first to provide evidence that extracellular ENO1 could enhance the intracellular glycolytic pathway. Studies of two cancer types, MM (the present study) and PCa (12) have been conducted, where high prevalence of ENO1 expression has been correlated to cancer progression (10,11). It was therefore conceivable that knockdown of ENO1 expression in both MM and PCa cells would lead to a decrease in pro-cancer

activities, as previously reported in other cancer types (5,18). However, it was surprising that extracellular ENO1 increased glycolysis (lactate production and LDH activity), cell viability, cell migration and the production of VEGF in the present study. In addition, the present study revealed that the extracellular ENO1-induced glycolysis and pro-cancer activities were mediated by the upregulated expression of HIF-1α and its downstream glycolysis-related proteins, HK2 and GLUT1.

Notably, it was demonstrated in the present study that enzymatic activity of administered extracellular ENO1 was not required for the glycolysis, cell migration and VEGF production induced by extracellular ENO1. It has also been previously reported that ENO1 enzymatic activity was not essential for the enhanced cell invasion and proliferation in lung cancer (18). These results therefore exclude the possibility that extracellular ENO1 enters the cytosol to directly enhance glycolysis with its enzymatic activity. However, the authors were unable to address the issue that if free unbound ENO1 in the medium could have any effect on glycolysis in their experiment settings. The use of an ENO1 mAb in the present study further demonstrated that surface ENO1 of MM or PCa (following stimulation with TNF-α) cells enhanced glycolysis, cell viability, cell migration and the production of VEGF and TGF-β. The ENO1 mAb suppressed glycolysis and pro-cancer activities by decreasing protein expression of HIF-1α and GRGs, such as HK2 and PFKFB3. Lastly, the results of the present study demonstrated that the ENO1 mAb inhibited MM tumor growth in nude mice and reduced the elevated serum lactate. The elevated serum lactate levels observed in the MM mice were associated with tumor growth, which was indicated by the increased lactate levels and tumor weight upon withdrawing of ENO1 mAb treatment.

Normal cells typically catabolize glucose by oxidative phosphorylation in the mitochondria, whereas tumor cells tend to convert glucose into lactate even in conditions of sufficient oxygen (36). This phenomenon was first studied by Otto Warburg and termed aerobic glycolysis or the Warburg effect (37). This reprogramming of energy metabolism has emerged as another hallmark of cancer (38). The upregulation of HIF-1α, numerous glycolytic enzymes (including LDH, PFK, HK2 and ENO1) or molecules associated with glucose uptake (such as GLUT1) have been reported in numerous types of cancer (39). HIF-1α regulation involves PHD, which induces HIF-1α degradation in normoxia, but allows stabilization of HIF-1α in hypoxia. However, in certain circumstances, HIF-1α regulation involves PHD-independent mechanism (40). Interestingly, it was identified that extracellular ENO1 had no significant impact on the regulation of PHD protein expression, and thus it was suggested by the authors that extracellular ENO1 could promote the HIF-1α protein expression through a PHD-independent mechanism. Moreover, it was investigated if HIF-1α expression could be regulated by ENO1 mAb under low oxygen or $CoCl_2$-mimicked condition. However, the authors' studies could not lead to consistent results so far from these two experimental systems. Efforts have been made to develop inhibitors to the aforementioned molecules (41), including intracellular ENO1 (42). However, no satisfactory clinical development to treat cancer by targeting the Warburg effect has been achieved, due to dose-limiting toxicities, low specificity and low potency of drugs (43). Although glycolysis is an ideal target pathway for cancer therapy, avoiding the risk of shutting down

glycolysis in all cells remains challenging. In the present study, it was demonstrated that surface ENO1 enhanced the glycolytic pathway in cancer cells, which makes the ENO1 antibody an ideal modality for targeting glycolysis in cancer cells expressing high levels of surface ENO1, such as in MM (11).

Lactate, the metabolic intermediate generated during aerobic glycolysis, is not only utilized as a fuel for growth but also provides acidity to the TME, which promotes the invasion and metastasis of cancer cells (44). Elevated lactate levels can inhibit the function of a variety of immune cells, such as T cells and natural killer cells (45). Certain strategies have been developed to target lactate production, such as inhibition of monocarboxylate transporters (46) and pyruvate dehydrogenase kinase-1 (47). It has also been reported that knockdown of the *ENO1* gene could reduce the production of lactate (48). The present study demonstrated that the HuniLife proprietary ENO1 mAb reduced lactate production and LDH activity in MM cells, which suggested a novel and feasible approach to regulate the TME.

It has previously been reported that aerobic glycolysis signatures were correlated with drug resistance in MM (49), and LDH A and HIF-1α were identified as valid targets to prevent MM drug resistance and progression *in vivo* (49). Moreover, HK2 was found to be upregulated in MM, which was significantly correlated with poor prognosis (50). Surface ENO1 was significantly upregulated in MM cells from patients, particularly after stimulation by pDCs in the TME (bone marrow) (11). The results of the present study indicated that the ENO1 mAb downregulated HIF-1α and HK2 protein expression, therefore the therapeutic potential of the ENO1 mAb in a clinical setting can be anticipated. In line with the aforementioned observations, in the present study, administration of extracellular ENO1 to MM cell culture increased HIF-1α and HK2 expression, and ENO1 mAb administration inhibited HIF-1α and HK2 expression in the absence of an additional source of ENO1. However, it remains difficult to reconcile the observations regarding the regulation of other glycolytic enzymes with these experimental results. In the present study, GLUT1 expression increased upon the addition of extracellular ENO1, while ENO1 mAb treatment of MM cells reduced the expression of PFKFB3 but not GLUT1. An improved understanding of the underlying mechanism of extracellular ENO1-regulated glycolysis is required to improve interpretation of these results.

The HuniLife proprietary ENO1 mAb was originally selected for its inhibitory activity on plasmin activation (close to 100%) in LPS-stimulated monocyte cells (U937), and it also exhibited an inhibitory activity (about 65.5±0.3%) against the invasion capabilities of ENO1-expressing lung cancer cells (CL1-5) (Patent: PCT/US2013/076877). The present study further demonstrated that the ENO1 mAb inhibited glycolysis via HIF-1α and glycolysis-related proteins in MM cells, but the detailed mechanisms by which ENO1 mAb regulates HIF-1α remain to be elucidated. The involvement of surface ENO1 in the uPAR/plasmin pathway added further complexity to the mechanism of study (51). It was hypothesized that the mechanism may involve ENO1-associated proteins on the cell surface, such as the hepatocytes growth factor receptor (HGFR) (18), B7-H3 (52) or fibroblast activation protein α (FAP) (9). Notably, B7-H3 promotes aerobic glycolysis by regulating HK2 (53), which coincides with the observation

in the present study that ENO1 mAb downregulates HK2 expression. Further investigation of the regulation of HIF-1α expression by surface ENO1 in other ENO1-related signaling pathways, including the HGFR-mediated PI3K/AKT and Wnt/β-catenin pathways or FAP-mediated NF-kB, is required.

A previous study demonstrated that the ENO1 mAb targeted multiple TME niches involved in PCa progression and bone metastasis (12). In the present study, the ENO1 mAb significantly reduced tumor growth in a MM subcutaneous xenograft mouse model. Indeed, there is a limitation on subcutaneous xenograft mouse model for the efficacy studies. However, the FDA-approved MM drugs, such as bortezomib (54) and daratumumab (55), all have demonstrated favorable efficacy in shrinking tumor in MM xenograft mice, indicating that such animal model still have clinical relevance to screening potential new drugs. The ENO1 mAb also reduced the viability of MM cells *in vitro*, but this reduction effect was modest even with statistical significance. By contrast, the ENO1 mAb had a marked inhibitory effect on tumor growth *in vivo*, suggesting that the anticancer mechanism of the ENO1 mAb may involve not only cancer cells but also TME niches (12). Therefore, it was reasonably suggested that the tumor inhibition activity of ENO1 mAb could result from its effects on TME, owing to its cross reactivity to mouse. MM cells grow in hypoxic niches inside the bone marrow with a metabolic shift towards aerobic glycolysis (56). Inhibition of ENO1 activates pDCs in the bone marrow microenvironment, leading to enhanced MM cell cytotoxicity (11). In addition, ENO1 is expressed in the cytosol and on the cell surface and can be found in the secretome (57). In the present study, it was shown that the addition of ENO1 (as a mimic of secreted protein) enhanced glycolytic activity through HIF-1α, and this enhancing effect was attenuated by the administration of ENO1 mAb. These data therefore provide evidence of a role of extracellular ENO1 (surface or secreted forms) in glycolytic modulation, and also provide the preclinical rationale for targeting extracellular ENO1-mediated metabolic reprogramming in cancer cells and the TME.

There are several notable observations regarding cytosolic or extracellular ENO1. Firstly, cytosolic ENO1 is highly expressed and utilized for glycolysis in cancer cells (48). Secondly, ENO1 is transported onto the cell surface of cancer cells (8) or activated immune cells (7), which activates plasmin to facilitate cell motility. Thirdly, the ENO1-induced biological activities are all related to cell survival, such as viability, motility, angiogenesis, cytokine and chemokine production, and energy programing (10). Based on the observation that extracellular ENO1 can promote glycolysis reprograming, it is conceivable that ENO1 may play a pivotal role in responding to stressed or hypoxic conditions, such as overgrown tumor cells in inflammatory and necrotic milieu.

In conclusion, the present study revealed an unexpected role of extracellular ENO1 in the crosstalk with the intracellular glycolytic pathway via HIF-1α (Fig. 7). However, the coordination and synchronicity of extracellular/intracellular ENO1 in regulating energy programs and ensuing biological activities in response to the ever-changing cellular environment remains to be elucidated. In summary, in the present study, the HuniLife ENO1-targeting antibody demonstrated multiple anticancer mechanisms via inhibition of glycolysis, lactate production, cytokine secretion, cell viability and migration.

This ENO1 antibody is currently in a phase I clinical trial for safety assessment, and future clinical studies are required to validate its anticancer potential in treating patients.

Availability of data and materials

The datasets used and/or analyzed during the current study are available from the corresponding author on reasonable request.

Authors' contributions

ICC, WCH and TTY conceived the study, wrote the original draft, reviewed and edited the manuscript. ICC, WCH, YTH, MLC, AWT and PYW collected, analyzed and interpreted the data. TTY supervised the study and acquired funding. MLC and AWT confirm the authenticity of all the raw data. All authors read and approved the final version of the manuscript.

Ethics approval and consent to participate

All animal studies were reviewed and approved by The Ethics Committee of TFBS Bioscience (Taipei, Taiwan). All animal procedures were performed according to approved protocols from the Institutional Animal Care and Use Committee (IACUC) of TFBS Bioscience (IACUC protocol no. TFBS2021-013).

Patient consent for publication

Not applicable.

Competing interests

The authors declare that they have no competing interests.

References

1. Didiasova M, Schaefer L and Wygrecka M: When place matters: Shuttling of enolase-1 across cellular compartments. Front Cell Dev Biol 7: 61, 2019.
2. Wold F and Ballou CE: Studies on the enzyme enolase. II. Kinetic studies. J Biol Chem 227: 313-328, 1957.
3. Vander Heiden MG, Cantley LC and Thompson CB: Understanding the Warburg effect: The metabolic requirements of cell proliferation. Science 324: 1029-1033, 2009.
4. Feron O: Pyruvate into lactate and back: from the Warburg effect to symbiotic energy fuel exchange in cancer cells. Radiother Oncol 92: 329-333, 2009.
5. Zhang J, Li H, Miao L and Ding J: Silencing of ENO1 inhibits the proliferation, migration and invasion of human breast cancer cells. J BUON 25: 696-701, 2020.
6. Plow EF and Das R: Enolase-1 as a plasminogen receptor. Blood 113: 5371-5372, 2009.
7. Wygrecka M, Marsh LM, Morty RE, Henneke I, Guenther A, Lohmeyer J, Markart P and Preissner KT: Enolase-1 promotes plasminogen-mediated recruitment of monocytes to the acutely inflamed lung. Blood 113: 5588-5598, 2009.
8. Principe M, Ceruti P, Shih NY, Chattaragada MS, Rolla S, Conti L, Bestagno M, Zentilin L, Yang SH, Migliorini P, et al: Targeting of surface alpha-enolase inhibits the invasiveness of pancreatic cancer cells. Oncotarget 6: 11098-11113, 2015.
9. Yuan Z, Hu H, Zhu Y, Zhang W, Fang Q, Qiao T, Ma T, Wang M, Huang R, Tang Q, et al: Colorectal cancer cell intrinsic fibroblast activation protein alpha binds to Enolase1 and activates NF-κB pathway to promote metastasis. Cell Death Dis 12: 543, 2021.
10. Almaguel FA, Sanchez TW, Ortiz-Hernandez GL and Casiano CA: Alpha-enolase: Emerging tumor-associated antigen, cancer biomarker, and oncotherapeutic target. Front Genet 11: 614726, 2020.
11. Ray A, Song Y, Du T, Chauhan D and Anderson KC: Preclinical validation of alpha-enolase (ENO1) as a novel immunometabolic target in multiple myeloma. Oncogene 39: 2786-2796, 2020.
12. Chen ML, Yuan TT, Chuang CF, Huang YT, Chung IC and Huang WC: A novel enolase-1 antibody targets multiple inter-acting players in the tumor microenvironment of advanced prostate cancer. Mol Cancer Ther 21: 1337-1347, 2022.
13. Sung H, Ferlay J, Siegel RL, Laversanne M, Soerjomataram I, Jemal A and Bray F: Global cancer statistics 2020: GLOBOCAN estimates of incidence and mortality worldwide for 36 cancers in 185 countries. CA Cancer J Clin 71: 209-249, 2021.
14. Kropff MH, Bisping G, Wenning D, Volpert S, Tchinda J, Berdel WE and Kienast J: Bortezomib in combination with dexamethasone for relapsed multiple myeloma. Leuk Res 29: 587-590, 2005.
15. Kumar S and Rajkumar SV: Thalidomide and lenalidomide in the treatment of multiple myeloma. Eur J Cancer 42: 1612-1622, 2006.
16. Lokhorst HM, Plesner T, Laubach JP, Nahi H, Gimsing P, Hansson M, Minnema MC, Lassen U, Krejcik J, Palumbo A, et al: Targeting CD38 with daratumumab monotherapy in multiple myeloma. N Engl J Med 373: 1207-1219, 2015.
17. Gou Y, Li F, Huo X, Hao C, Yang X, Pei Y, Li N, Liu H and Zhu B: ENO1 monoclonal antibody inhibits invasion, prolifera-tion and clone formation of cervical cancer cells. Am J Cancer Res 11: 1946-1961, 2021.
18. Li HJ, Ke FY, Lin CC, Lu MY, Kuo YH, Wang YP, Liang KH, Lin SC, Chang YH, Chen HY, et al: ENO1 promotes lung cancer metastasis via HGFR and WNT signaling-driven epithe-lial-to-mesenchymal transition. Cancer Res 81: 4094-4109, 2021.
19. Shu X, Cao KY, Liu HQ, Yu L, Sun LX, Yang ZH, Wu CA and Ran YL: Alpha-enolase (ENO1), identified as an antigen to monoclonal antibody 12C7, promotes the self-renewal and malignant phenotype of lung cancer stem cells by AMPK/mTOR pathway. Stem Cell Res Ther 12: 119, 2021.
20. Hsiao KC, Shih NY, Fang HL, Huang TS, Kuo CC, Chu PY, Hung YM, Chou SW, Yang YY, Chang GC and Liu KJ: Surface α-enolase promotes extracellular matrix degradation and tumor metastasis and represents a new therapeutic target. PLoS One 8: e69354, 2013.
21. Yu L, Shi J, Cheng S, Zhu Y, Zhao X, Yang K, Du X, Klocker H, Yang X and Zhang J: Estrogen promotes prostate cancer cell migration via paracrine release of ENO1 from stromal cells. Mol Endocrinol 26: 1521-1530, 2012.
22. Fujiwara S, Wada N, Kawano Y, Okuno Y, Kikukawa Y, Endo S, Nishimura N, Ueno N, Mitsuya H and Hata H: Lactate, a putative survival factor for myeloma cells, is incorporated by myeloma cells through monocarboxylate transporters 1. Exp Hematol Oncol 4: 12, 2015.
23. Samec M, Liskova A, Koklesova L, Mersakova S, Strnadel J, Kajo K, Pec M, Zhai K, Smejkal K, Mirzaei S, et al: Flavonoids targeting HIF-1: Implications on cancer metabolism. Cancers (Basel) 13: 130, 2021.
24. Qiao G, Wu A, Chen X, Tian Y and Lin X: Enolase 1, a moon-lighting protein, as a potential target for cancer treatment. Int J Biol Sci 17: 3981-3992, 2021.
25. Zakrzewicz D, Didiasova M, Krüger M, Giaimo BD, Borggrefe T, Mieth M, Hocke AC, Zakrzewicz A, Schaefer L, Preissner KT and Wygrecka M: Protein arginine methyltransferase 5 mediates enolase-1 cell surface trafficking in human lung adenocarcinoma cells. Biochim Biophys Acta Mol Basis Dis 1864: 1816-1827, 2018.

26. Livak KJ and Schmittgen TD: Analysis of relative gene expression data using real-time quantitative PCR and the 2(-Delta Delta C(T)) method. Methods 25: 402-408, 2001.
27. Fu QF, Liu Y, Fan Y, Hua SN, Qu HY, Dong SW, Li RL, Zhao MY, Zhen Y, Yu XL, et al: Alpha-enolase promotes cell glycolysis, growth, migration, and invasion in non-small cell lung cancer through FAK-mediated PI3K/AKT pathway. J Hematol Oncol 8: 22, 2015.
28. Song Y, Luo Q, Long H, Hu Z, Que T, Zhang X, Li Z, Wang G, Yi L, Liu Z, et al: Alpha-enolase as a potential cancer prognostic marker promotes cell growth, migration, and invasion in glioma. Mol Cancer 13: 65, 2014.
29. El Arfani C, De Veirman K, Maes K, De Bruyne E and Menu E: Metabolic features of multiple myeloma. Int J Mol Sci 19: 1200, 2018.
30. Ahmad F, Cherukuri MK and Choyke PL: Metabolic reprogramming in prostate cancer. Br J Cancer 125: 1185-1196, 2021.
31. Hamaguchi T, Iizuka N, Tsunedomi R, Hamamoto Y, Miyamoto T, Iida M, Tokuhisa Y, Sakamoto K, Takashima M, Tamesa T and Oka M: Glycolysis module activated by hypoxia-inducible factor 1alpha is related to the aggressive phenotype of hepatocellular carcinoma. Int J Oncol 33: 725-731, 2008.
32. Cippitelli M, Stabile H, Kosta A, Petillo S, Lucantonio L, Gismondi A, Santoni A and Fionda C: Role of NF-κB signaling in the interplay between multiple myeloma and mesenchymal stromal cells. Int J Mol Sci 24: 1823, 2023.
33. Wei Y, Xu H, Dai J, Peng J, Wang W, Xia L and Zhou F: Prognostic significance of serum lactic acid, lactate dehydrogenase, and albumin levels in patients with metastatic colorectal cancer. Biomed Res Int 2018: 1804086, 2018.
34. Vlachostergios PJ, Oikonomou KG, Gibilaro E and Apergis G: Elevated lactic acid is a negative prognostic factor in metastatic lung cancer. Cancer Biomark 15: 725-734, 2015.
35. Glassman PM and Balthasar JP: Mechanistic considerations for the use of monoclonal antibodies for cancer therapy. Cancer Biol Med 11: 20-33, 2014.
36. Koppenol WH, Bounds PL and Dang CV: Otto Warburg's contributions to current concepts of cancer metabolism. Nat Rev Cancer 11: 325-337, 2011.
37. Warburg O, Wind F and Negelein E: The Metabolism of tumors in the body. J Gen Physiol 8: 519-530, 1927.
38. Schwartz L, Supuran CT and Alfarouk KO: The Warburg effect and the hallmarks of cancer. Anticancer Agents Med Chem 17: 164-170, 2017.
39. Yu L, Chen X, Wang L and Chen S: The sweet trap in tumors: Aerobic glycolysis and potential targets for therapy. Oncotarget 7: 38908-38926, 2016.
40. Iommarini L, Porcelli AM, Gasparre G and Kurelac I: Non-canonical mechanisms regulating hypoxia-inducible factor 1 alpha in cancer. Front Oncol 7: 286, 2017.
41. Chen XS, Li LY, Guan YD, Yang JM and Cheng Y: Anticancer strategies based on the metabolic profile of tumor cells: Therapeutic targeting of the Warburg effect. Acta Pharmacol Sin 37: 1013-1019, 2016.
42. Lung J, Chen KL, Hung CH, Chen CC, Hung MS, Lin YC, Wu CY, Lee KD, Shih NY and Tsai YH: In silico-based identification of human α-enolase inhibitors to block cancer cell growth metabolically. Drug Des Devel Ther 11: 3281-3290, 2017.
43. Galluzzi L, Kepp O, Vander Heiden MG and Kroemer G: Metabolic targets for cancer therapy. Nat Rev Drug Discov 12: 829-846, 2013.
44. de la Cruz-López KG, Castro-Muñoz LJ, Reyes-Hernández DO, García-Carrancá A and Manzo-Merino J: Lactate in the regulation of tumor microenvironment and therapeutic approaches. Front Oncol 9: 1143, 2019.
45. Brand A, Singer K, Koehl GE, Kolitzus M, Schoenhammer G, Thiel A, Matos C, Bruss C, Klobuch S, Peter K, et al: LDHA-associated lactic acid production blunts tumor immunosurveillance by T and NK cells. Cell Metab 24: 657-671, 2016.
46. Goodwin ML, Gladden LB, Nijsten MWN and Jones KB: Lactate and cancer: Revisiting the warburg effect in an era of lactate shuttling. Front Nutr 1: 27, 2015.
47. Fujiwara S, Kawano Y, Yuki H, Okuno Y, Nosaka K, Mitsuya H and Hata H: PDK1 inhibition is a novel therapeutic target in multiple myeloma. Br J Cancer 108: 170-178, 2013.
48. Capello M, Ferri-Borgogno S, Riganti C, Chattaragada MS, Principe M, Roux C, Zhou W, Petricoin EF, Cappello P and Novelli F: Targeting the Warburg effect in cancer cells through ENO1 knockdown rescues oxidative phosphorylation and induces growth arrest. Oncotarget 7: 5598-5612, 2016.
49. Maiso P, Huynh D, Moschetta M, Sacco A, Aljawai Y, Mishima Y, Asara JM, Roccaro AM, Kimmelman AC and Ghobrial IM: Metabolic signature identifies novel targets for drug resistance in multiple myeloma. Cancer Res 75: 2071-2082, 2015.
50. Nakano A, Miki H, Nakamura S, Harada T, Oda A, Amou H, Fujii S, Kagawa K, Takeuchi K, Ozaki S, et al: Up-regulation of hexokinaseII in myeloma cells: Targeting myeloma cells with 3-bromopyruvate. J Bioenerg Biomembr 44: 31-38, 2012.
51. Gonias SL and Hu J: Urokinase receptor and resistance to targeted anticancer agents. Front Pharmacol 6: 154, 2015.
52. Zuo J, Wang B, Long M, Gao Z, Zhang Z, Wang H, Wang X, Li R, Dong K and Zhang H: The type 1 transmembrane glycoprotein B7-H3 interacts with the glycolytic enzyme ENO1 to promote malignancy and glycolysis in HeLa cells. FEBS Lett 592: 2476-2488, 2018.
53. Shi T, Ma Y, Cao L, Zhan S, Xu Y, Fu F, Liu C, Zhang G, Wang Z, Wang R, et al: B7-H3 promotes aerobic glycolysis and chemoresistance in colorectal cancer cells by regulating HK2. Cell Death Dis 10: 308, 2019.
54. Ishii T, Seike T, Nakashima T, Juliger S, Maharaj L, Soga S, Akinaga S, Cavenagh J, Joel S and Shiotsu Y: Anti-tumor activity against multiple myeloma by combination of KW-2478, an Hsp90 inhibitor, with bortezomib. Blood Cancer J 2: e68, 2012.
55. Sanchez L, Wang Y, Siegel DS and Wang ML: Daratumumab: A first-in-class CD38 monoclonal antibody for the treatment of multiple myeloma. J Hematol Oncol 9: 51, 2016.
56. Storti P, Bolzoni M, Donofrio G, Airoldi I, Guasco D, Toscani D, Martella E, Lazzaretti M, Mancini C, Agnelli L, et al: Hypoxia-inducible factor (HIF)-1α suppression in myeloma cells blocks tumoral growth in vivo inhibiting angiogenesis and bone destruction. Leukemia 27: 1697-1706, 2013.
57. de Oliveira G, Freire PP, Cury SS, de Moraes D, Oliveira JS, Dal-Pai-Silva M, Reis PP and Carvalho RF: An integrated meta-analysis of secretome and proteome identify potential biomarkers of pancreatic ductal adenocarcinoma. Cancers (Basel) 12: 716, 2020.